# Plasma-wall transition in weakly collisional plasmas

Giovanni Manfredi, Stéphane Devaux

# Plasma-wall transition in weakly collisional plasmas

G. Manfredi* and S. Devaux†

*Institut de Physique et Chimie des Matériaux de Strasbourg, BP 43, F-67034 Strasbourg, France
†Laboratoire de Physique des Milieux Ionisés et Applications, Université Henri Poincaré, F-54506 Vandoeuvre-les-Nancy, France

**Abstract.** This paper reviews some theoretical and computational aspects of plasma-wall interactions, in particular the formation of sheaths. Some fundamental results are derived analytically using a simple fluid model, and are subsequently tested with kinetic simulations. The various regions composing the plasma-wall transition (Debye sheath, collisional and magnetic presheaths) are discussed in details.

**Keywords:** Plasma-wall interactions, kinetic modeling, Vlasov codes
**PACS:** 52.40.Kh, 52.65.-y, 52.25.Dg

## 1. INTRODUCTION

The interaction of a plasma with a surface is one of the oldest problems in plasma physics. This is hardly surprising, as any plasma created in the laboratory needs to be confined by a material vessel. Besides, a large number of diagnostics are obtained with probes inserted into the plasma, thus exposing some solid surface to the charged particles.

Perhaps the most distinctive character of plasma-wall interaction is that solid surfaces act as sinks and sources for the plasma. When an ion hits the surface, it is usually retained on it for a time sufficiently long to recombine with the electrons on the surface. The atoms thus formed are usually weakly bounded to the surface and are re-emitted as neutrals into the plasma. Subsequently, these neutrals can be re-ionized, generally by electron impact. Besides, electrons can also be emitted from the surface by impact of other particles. This process of recombination/emission/ionization can lead to a steady-state regime named recycling [1].

A second, and most important, effect caused by the presence of a solid surface is the formation of plasma sheaths, i.e. boundary layers that allow a smooth transition between the bulk plasma (at thermodynamic equilibrium) and the surface. For magnetized plasmas, at least three layers can be identified. Proceeding from the bulk plasma to the wall we find: (i) the quasineutral collisional/ionizing presheath (CP); (ii) the magnetic presheath (MP), also quasineutral; and (iii) the electrically charged Debye sheath (DS). These regions are dominated by different physical effects and are characterized by disparate length scales, which makes the numerical modelling of the entire transition a particularly difficult task.

Potential applications of plasma-wall interaction are ubiquitous and many of them are related to magnetically confined fusion plasmas. The plasma is confined by strong

CP1061, *Frontiers in Modern Plasma Physics*, edited by P. K. Shukla, B. Eliasson, and L. Stenflo

magnetic fields in a toroidal chamber (tokamak). However, radial transport cannot be completely suppressed, and the charged particles escaping the confinement must be redirected towards some solid targets (limiters, divertors) specifically designed to support large fluxes. Sputtering of these devices can end up in significant erosion of their surfaces. Meanwhile, sputtered atoms can leave the surface and enter the plasma, leading to its contamination [1].

Further applications of plasma-wall interactions come from probe theory. Probes are routinely used for tokamak edge measurements, though their results are notoriously difficult to interpret, because the very presence of the probe can perturb the ambient plasma by creating a sheath. It is therefore of paramount importance to assess the properties of the sheath in order to relate the quantities measured by the probe to those of the unperturbed plasma [2].

## 2. UNMAGNETIZED PLASMA-WALL TRANSITION

When a material object comes in contact with a warm electron-ion plasma, both species are collected at the object's surface. However, the ions and the electrons hit the surface at very different rates, roughly proportional to their thermal speeds, which scale as the square root of the ion-to-electron mass ratio. Then, a negative charge accumulates on the wall, which in turn will be screened by a positive charge developing in its vicinity. This region of the plasma (called the Debye sheath, or simply the sheath) has a thickness of the order of the Debye length and is essentially collisionless.

In order for the plasma-wall transition to be stable, the ions must enter the DS with a velocity larger than the ion sound speed, a condition known as *Bohm's criterion* [3]. This can be easily proven using a fluid model and searching for stationary solutions, which must satisfy the continuity and Euler equations for the ion density $n_i(x)$ and mean velocity $u_i(x)$:

$$\frac{d(n_i u_i)}{dx} = S, \tag{1}$$

$$n_i m_i u_i \frac{du_i}{dx} = -e n_i \frac{d\phi}{dx} - m_i u_i S. \tag{2}$$

Here, the ions are supposed to be cold ($T_i = 0$), the electrons follow the Boltzmann relation $n_e = n_0 \exp(e\phi/k_B T_e)$, $S(x)$ denotes a generic source that models collisions and/or ionization, and $\phi$ is the electrostatic potential obeying Poisson's equation

$$\varepsilon_0 \frac{d^2\phi}{dx^2} = -e(n_i - n_e). \tag{3}$$

In the DS, collisions and ionization are negligible, therefore we set $S = 0$. Equations (1)-(2) can thus be integrated exactly between the entrance of the DS (denoted by the subscript "ds") and a generic position $x$. We easily obtain the relation $n_i/n_{ds} = [1 - 2e(\phi - \phi_{ds})/m_i u_{ds}^2]^{-1/2}$. Substituting this expression in Poisson's equation (3) and linearizing (i.e. assuming that $e(\phi - \phi_{ds})$ is much smaller than both $k_B T_e$ and $m_i u_{ds}^2$),

yields the following result

$$\frac{d^2\phi}{dx^2} = \frac{1}{\lambda_{De}^2}\left(1 - \frac{k_B T_e}{m_i u_{ds}^2}\right)\phi, \tag{4}$$

where $\lambda_{De} = \sqrt{\varepsilon_0 k_B T_e / e^2 n_0}$ is the Debye length. In order for Eq. (4) to support monotonic solutions, one must satisfy

$$u_{ds} \geq c_s \equiv \sqrt{\frac{k_B T_e}{m_i}}, \tag{5}$$

which is the expected Bohm criterion. Further considering the linearized Eq. (4), we see that the solution is an exponential function with characteristic length close to the Debye length (as long as the electron temperature is not too high), which thus represents the typical thickness of the DS.

We now turn to the region between the bulk plasma and the DS entrance, which is usually referred to as the *collisional presheath* (CP), because we expect collisions and ionization to play a crucial role, so that $S \neq 0$. We also assume the CP to be quasineutral, and therefore the relation $n_i = n_e \equiv n$ replaces Poisson's equation (3). After some algebra, Eqs. (1)-(2) can be reformulated in terms of the Mach number $M(x) = u_i(x)/c_s$, which obeys the equation

$$\frac{dM}{dx} = \frac{S}{n c_s}\frac{(1+M^2)}{(1-M^2)}. \tag{6}$$

We see immediately that a singularity appears at $M = 1$, i.e. for a velocity equal to the ion sound speed. The singularity corresponds to the entrance of the DS, where Bohm's criterion starts being verified. The singularity signals that the assumption of quasineutrality is no longer valid, and must be replaced with the full Poisson's equation, as was done for the treatment of the DS. As the right-hand side of Eq. (6) is always positive, the Mach number grows monotonically in the CP region from its value in the bulk plasma (which can be nonzero, as flows are frequently present in tokamak edge plasmas) up to the value $M = 1$ at the entrance of the DS.

For simplicity, we take a source term of the form $S(x) = n/\tau_{\text{coll}}$, where $\tau_{\text{coll}}$ is a typical relaxation time. In this case, Eq. (6) can be integrated exactly, yielding the relation: $2\arctan M - M = x/(\tau_{\text{coll}} c_s)$. In the bulk plasma (located at $x = 0$), we can take $M = 0$, whereas at the DS entrance ($x = L$) Bohm's criterion implies that $M = 1$. This yields $L = (\pi/2 - 1)\tau_{\text{coll}} c_s$, which confirms that the thickness $L$ of the CP is of the order of the collisional mean free path $\lambda_{\text{mfp}} = \tau_{\text{coll}} c_s$.

We can now establish a relationship between the Mach number and the particle density in the CP. By eliminating the source from Eqs. (1)-(2), we obtain the energy conservation relation: $n k_B T_e + m_i n v^2 = \text{const}$. The integration constant is fixed so that $n = n_0$ when $u = 0$, which yields, in terms of the Mach number

$$n(x) = \frac{n_0}{1 + M^2(x)}, \tag{7}$$

and for the potential, using the Boltzmann relation: $e\phi = -k_B T_e \ln(1 + M^2)$. Therefore, at the boundary between the CP and the DS (where $M = 1$), the density and the potential

obey the simple relations: $n = n_0/2$ and $e\phi = -\ln(2) k_B T_e \simeq -0.7 k_B T_e$. We also emphasize that the above results do not change if the ion temperature is taken into account, provided that the sound speed is defined using the total (ion and electron) temperature.

It is also possible to estimate the value of the electric potential on the wall. At the DS entrance, in virtue of Eq. (7), the ion flux can be estimated as: $\Gamma_i = n_0 c_s/2$. This value also represents the ion flux at the wall, because the flux is conserved in the collisionless DS. The electron flux can be estimated by assuming that the electron distribution on the wall is a half-Maxwellian, which yields:

$$\Gamma_e = n_0 \left( \frac{k_B T_e}{2\pi m_e} \right)^{1/2} \exp\left( \frac{e\phi_{\text{wall}}}{k_B T_e} \right). \tag{8}$$

By equating the ion and electron fluxes (ambipolarity), and allowing for a finite ion temperature in $c_s$, we obtain

$$\frac{e\phi_{\text{wall}}}{k_B T_e} = \frac{1}{2} \ln\left[ 2\pi \frac{m_e}{m_i} \left( 1 + \frac{T_i}{T_e} \right) \right]. \tag{9}$$

Due to the logarithm in Eq. (9), the dependence on both the temperature and mass ratios is rather weak. For instance, when $T_i = T_e$, we have for hydrogen, deuterium, tritium, and argon: $\phi^H_{\text{wall}} = -2.49$, $\phi^D_{\text{wall}} = -2.84$, $\phi^T_{\text{wall}} = -3.04$, and $\phi^{Ar}_{\text{wall}} = -4.33$ in units of $k_B T_e/e$. These value should be compared to the much smaller drop of the potential in the CP, which is roughly $-0.7 k_B T_e$, irrespective of the mass and temperature ratios.

Finally, we estimate the ion density on the wall by equating the ion flux at the wall to the ion flux at the DS entrance: $n_i^{\text{wall}} u_i^{\text{wall}} = n_0 c_s/2$. The ions velocity on the wall $u_i^{\text{wall}}$ is easily obtained using energy conservation in the DS. Finally, we obtain for the ion density

$$\frac{n_i^{\text{wall}}}{n_0} = \frac{1}{2} \left( 1 + \frac{2e\Delta\phi}{k_B T_e} \right)^{-1/2}, \tag{10}$$

where $\Delta\phi$ is the potential drop between the DS entrance and the wall.

**TABLE 1.** Densities, potential, and ion velocity at various points in the plasma-wall transition.

| | $n_i/n_0$ | $n_e/n_0$ | $e\phi/k_B T_e$ | $u_i/c_s$ |
|---|---|---|---|---|
| Bulk | 1 | 1 | 0 | 0 |
| DSE | 0.5 | 0.5 | −0.7 | 1 |
| Wall | 0.22 | 0.06 | −2.84 | 2.3 |

Table 1 summarizes the values of the densities, the electrostatic potential, and the ion velocity in the bulk plasma, at the DS entrance, and on the wall, for a deuterium plasma with $T_e = T_i$. It is clear that the main potential drop occurs in the DS, and that the DS is positively charged ($n_i > n_e$). The ion velocity becomes supersonic in the DS.

## 3. KINETIC MODELLING

The results of the preceding section were obtained with a simple fluid model, which makes the tacit assumption that the ion distribution is everywhere Maxwellian. This is

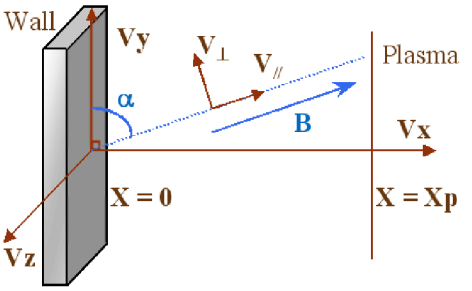


**FIGURE 1.** Geometry of the plasma-wall transition. The wall lies in the yOz plane, at $x = 0$, and the equilibrium plasma is located at $x \geq x_p$. The magnetic field, situated in the xOy plane, make an angle $\alpha$ with the wall.

known to be incorrect, particularly in the DS, where the strong electric fields deform substantially the ion distribution. A more realistic description should resort to *kinetic* modelling, by solving the relevant equation for the phase-space ion distribution function $f_i(\mathbf{r}, \mathbf{v}, t)$. The evolution of the distribution function is governed by a modified Vlasov equation that includes a collision term

$$\frac{\partial f_i}{\partial t} + v_x \frac{\partial f_i}{\partial x} + \frac{e}{m}(\mathbf{E} + \mathbf{v} \times \mathbf{B}) \cdot \frac{\partial f_i}{\partial \mathbf{v}} = -\nu_{\text{coll}}(f_i - f_0), \tag{11}$$

where $\nu_{\text{coll}}$ is the ion-neutral collision frequency (ion-ion and ion-electron collisions are neglected, as their mean free paths are significantly larger) and $\mathbf{E} = -\nabla\phi$ is the electric field. The electric potential obeys Poisson's equation (3), where the ion and electron densities are respectively $n_i = \int f_i dv$ and $n_e = n_0 \exp(e\phi/k_B T_e)$. The geometry of the simulations is shown in Fig. 1. The wall is located at $x = 0$ and is supposed to be perfectly absorbing. In the bulk plasma ($x \geq x_p$), the ion distribution is a Maxwellian $f_0(v)$ with equilibrium temperature $T_{i0}$ and density $n_0$.

The following boundary conditions are adopted for the Poisson equation: (i) on the plasma side ($x = x_p$), the potential is set to zero; (ii) at the wall ($x = 0$), a floating potential condition is assumed, given by the accumulation of electric charges on the wall. The floating potential is computed by integrating Ampère's equation on the wall:

$$\frac{\partial E_x}{\partial t} = -\frac{e}{\varepsilon_0}(\Gamma_i - \Gamma_e). \tag{12}$$

The ion flux towards the wall is equal to $\Gamma_i = \int v_x f_i \, d\mathbf{v}$, whereas the electron flux is given by Eq. (8).

As we are mainly interested in the steady-state solutions, we let the plasma evolve according to the Vlasov-Poisson equations until a stationary state is reached. The run is stopped when the spatial profiles of physically relevant quantities do not evolve any longer. The magnetic field $\mathbf{B}$, which is uniform and time-independent, makes an angle $\alpha$ with the wall. When the magnetic field is absent or is normal to the wall, the relevant phase space reduces to two dimensions $(x, v_x)$, whereas for oblique incidence the three components of the particle velocities need to be taken into account.

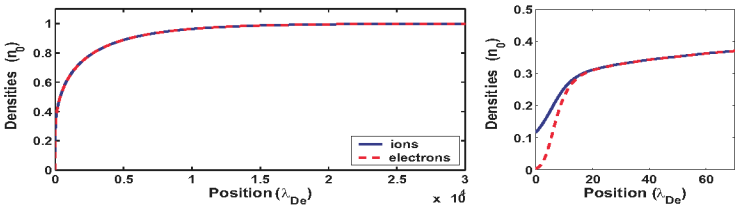


**FIGURE 2.** Density profiles in this entire transition region (left) and near the wall (right).

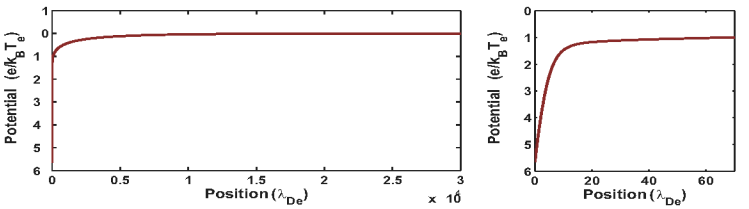


**FIGURE 3.** Electrostatic potential in this entire transition region (left) and near the wall (right).

The Vlasov equation is solved with an Eulerian code based on a fixed mesh covering the entire phase-space [4]. The time integration relies on a splitting scheme, which treats each phase space direction separately. This approach has the advantage of reducing the numerical noise compared to Particle-In-Cell (PIC) simulations. As several disparate length scales are present in the plasma-wall transition, we employ an inhomogeneous grid, which amounts to using a fine mesh in the DS (where gradients are steep) and a coarser one in the presheath.

## 4. NUMERICAL RESULTS

First, we consider the simpler case of an unmagnetized plasma. The typical profiles of the density and electrostatic potential in the CP and DS are shown on Figs. 2-3. The charge separation within the DS is clearly visible, and corresponds to the steepening of the electrostatic potential. Therefore, the electric field is much stronger in the DS than in the CP.

Figure 4 shows the Mach number at the entrance of the DS, for various values of the temperature ratio $\tau = T_e/T_i$ and collision frequency (normalized to the ion plasma frequency). The Bohm criterion is mostly satisfied, except for some cases at large collision frequency. This can be understood by noting that the effect of collisions is mainly to reconstruct the equilibrium Maxwellian $f_0$ on a time scale of the order of $\nu_{\rm coll}^{-1}$. This creates a tail of slow particles in the CP, as can be seen on Fig. 5 (top panel). If we compute the average velocity using the full ion distribution (Fig. 5, bottom frame, solid curve), Bohm's criterion is not satisfied, because the slow-particle tail reduces the value of the mean velocity. Instead, if we compute the ion velocity using only particles from the core of the distribution (represented by a dashed curve in the top panel of Fig. 5), the

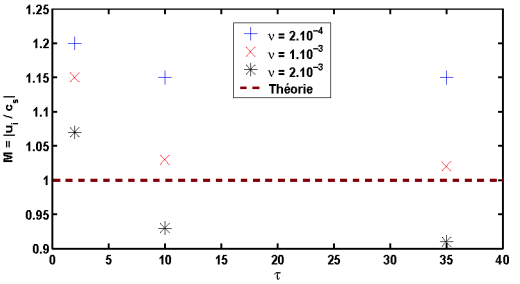


**FIGURE 4.** Mach number at the DS entrance vs. temperature ratio $\tau = T_e/T_i$, for various values of the normalized collision frequency. The straight dashed line corresponds to Bohm's criterion.

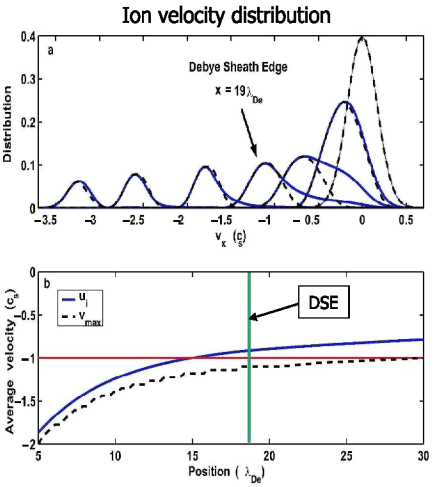


**FIGURE 5.** Top frame: ion velocity distribution at various points in the plasma-wall transition. Bottom frame: average velocity computed from the whole distribution (solid line) and after suppressing the slow-velocity tail (dashed line).

criterion is correctly verified (bottom panel, dashed curve).

From Fig. 5, we also see that the width of the ion velocity distribution increases considerably in the CP and the MP. This effect corresponds to an increase in the ion "temperature", defined as the variance of the velocity distribution. This kinetic temperature corresponds to the thermodynamic temperature only when the distribution is Maxwellian, which is not the case in the presheaths. In order to validate our model, we have tried to reproduce the ion temperature profile observed experimentally in Ref. [5]. The main parameters are as follows: $\tau = T_e/T_i = 25$, $\lambda_{\text{mfp}} = 10^4 \lambda_{Di}$, and wall polarization $\phi_w = -30V$. The result is presented in Fig. 6, for three different values of the collision rate normalized to the ion plasma frequency. The experimental value $\nu = 10^{-4}\omega_{pi}$ slightly overestimates the ion temperature, but the result is rather satisfactory for $\nu = 2 \times 10^{-4}\omega_{pi}$.

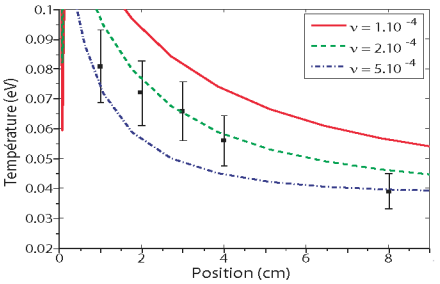


**FIGURE 6.** Ion temperature profile. Black dots: experimental results from Ref. [5]. Continuous lines: numerical results for various collisions rates normalized to $\omega_{pi}$.

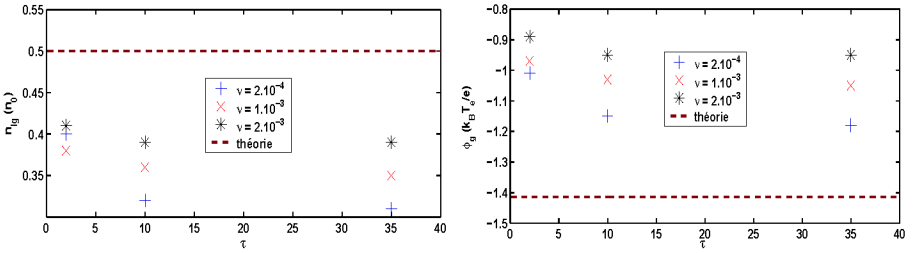


**FIGURE 7.** Ion density (left frame) and electrostatic potential (right frame) at the DS entrance, for various temperature ratios $\tau$ and normalized collision frequencies $\nu = \nu_{\rm coll}/\omega_{pi}$. Dashed lines are the theoretical estimates from fluid theory: $n = n_0/2$ and $e\phi = -\ln(2)k_BT_e \simeq -0.7k_BT_e$.

Figure 7 shows the ion density and the electrostatic potential at the DS entrance. The theoretical estimations obtained with the fluid model (Sec. 2) are not satisfied by a rather wide margin. It is clear, therefore, that a fluid approach, although it provides a qualitatively correct picture of the transition, cannot give quantitatively accurate results.

We now present some results for the magnetized transition. More details can be found in our recent publications [6, 7]. When a tilted magnetic field is present (Fig. 1), a third region arises in between the collisional presheath and the Debye sheath [8]: this is the magnetic presheath (MP), which is quasineutral and has an extension that scales like the ion Larmor radius $\rho_i$. The following ordering is assumed: $\lambda_{De} \ll \rho_i \ll \lambda_{\rm mfp}$, where $\lambda_{\rm mfp}$ is the ion-neutral mean free path. This ordering is valid for most low-pressure gas discharge experiments, and also for tokamak edge plasmas. Other possible scalings were considered by Ahedo [9].

The ion phase-space portraits in the plane $(v_x, v_y)$, where the magnetic field lies, are shown in Fig. 8. These show that the ions are first accelerated along the magnetic field lines in the CP ($x = 631\lambda_{Di}$); subsequently, in the MP, their velocity is redirected in the direction normal to the wall ($x = 196\lambda_{Di}$); finally, in the DS, the ions are strongly accelerated towards the wall ($x < 40\lambda_{Di}$).

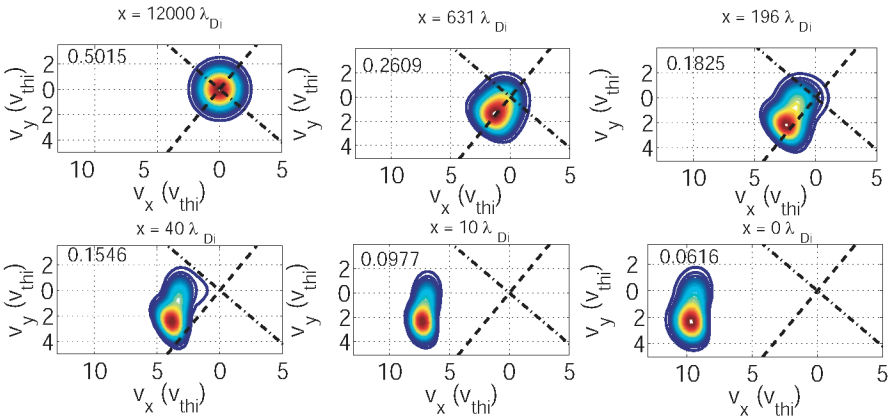


**FIGURE 8.** Contours of the ion distribution function in the $(v_x, v_y)$ plane for a magnetized case, with $\alpha = 40°$, $\omega_{ci}/\omega_{pi} = 0.01$, $\tau = 10$ and $\nu = 10^{-3}$. The top left panel corresponds to the bulk plasma ($x = 12000\lambda_{Di}$); the bottom right panel corresponds to the wall ($x = 0$).

The general structure of the magnetized plasma wall transition is represented in Fig. 9. The left frames of the figure show the entire transition, whereas the right frames show a zoom on the first 100 Debye lengths in front of the wall. Looking at the whole transition, it appears that a first separation into two different zones can be drawn approximately at $x \sim 600\lambda_{De}$. This correspond to the magnetic presheath edge (MPE). At the MPE, the density profiles become significantly steeper, although quasineutrality is still verified. In turn, the electrostatic potential also becomes steeper, thus signalling a stronger electric field in this region. Finally, we notice that, for $x > 600\lambda_{De}$, the velocity parallel to **B** deviates appreciably from zero, but not the perpendicular velocity: this reflects the fact that, in the CP, the ions are mainly accelerated along the magnetic field lines. The perpendicular velocity starts being different from zero at the MPE, where the ions are partially redirected towards the wall.

The zoom (right frames on Fig. 9) shows the transition between the MP and the DS, which occurs around $x = 20\lambda_{De}$. In the DS, quasineutrality is lost and the potential drops even further over a very thin region (thus, a strong electric field is present in the DS). The ions are further accelerated along the direction normal to the wall.

## 5. CONLUSION

In this paper we have presented a short overview of the physical issues of plasma-wall transition modelling. Fluid models provide a qualitatively correct picture of the transition (drop of the densities and electrostatic potential, ion acceleration), but neglect a number of important effects. In particular, they fall short of taking into account the considerable distortion of the ion distribution in the sheath and presheath. Here, we have developed a kinetic model based on the ion Vlasov equation, whereas the electrons are assumed to be at thermal equilibrium. The Vlasov equation was solved with an Eulerian

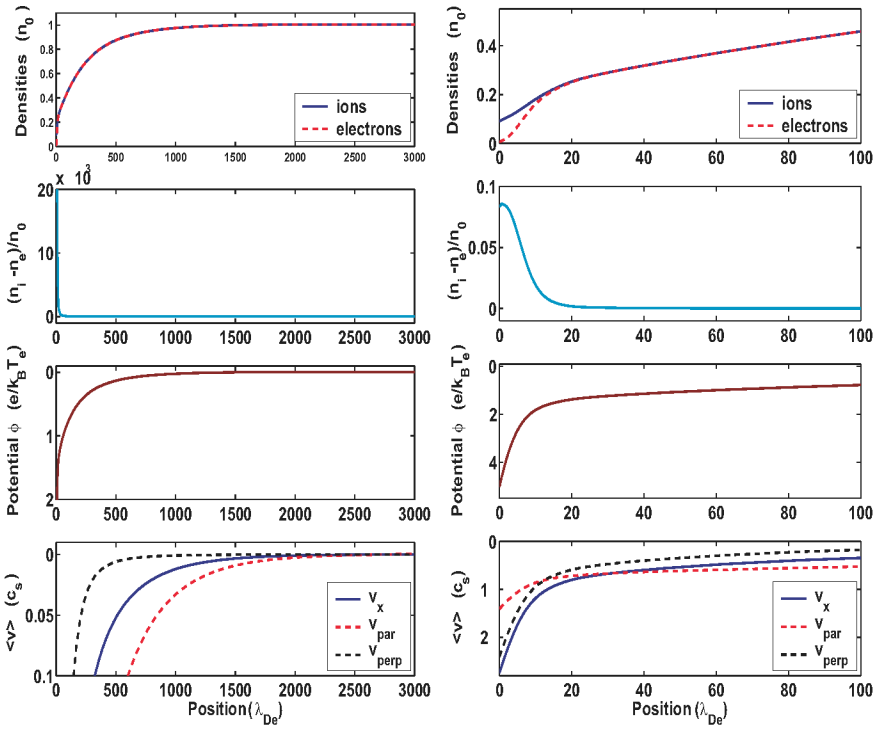


**FIGURE 9.** From top to bottom: densities, charge distribution, electrostatic potential, and ion velocity for a magnetized case with $\nu = 10^{-3}$, $\tau = 10$, $\omega_{ci}/\omega_{pi} = 0.01$ and $\alpha = 20°$. Left frames: entire transition; right frames: zoom near the wall.

code, which displays a fine resolution in phase space. The use of a nonuniform grid allowed an optimal description of the various regions, which are characterized by very disparate length scales. The numerical results provide a comprehensive picture of the plasma-wall transition, both with and without magnetic field.

## REFERENCES


1. P. C. Stangeby, *The plasma boundary of magnetic fusion devices* (IOP Publishing, London, 2000).
2. F. Valsaque, G. Manfredi, J.P. Gunn, E. Gauthier, Phys. Plasmas **9**, 1806 (2002).
3. D. Bohm, in *The Characteristics of Electrical Discharges in Magnetic Fields*, edited by A. Guthrie and R. K. Wakerling (McGraw-Hill, New York, 1949). See also: K.U. Riemann, J. Appl. Phys. D **24**, 493 (1991).
4. G. Manfredi and F. Valsaque, Comp. Phys. Comm. **164**, 262 (2004).
5. L. Oksuz and N. Hershkowitz, Plasma Sources Sci. Technol **16**, 201 (2003).
6. S. Devaux and G. Manfredi, Phys. Plasmas **13**, 083504 (2006);
7. S. Devaux and G. Manfredi, Plasma Phys. Control. Fus. **50**, 025009 (2008).
8. R. Chodura, Phys. Fluids **25**, 1628 (1982).
9. E. Ahedo, Phys. Plasmas **4**, 4419 (1997).